

Assessment of dispersion parameterizations through wind data measured by three sonic anemometers in a urban canopy

L. Mortarini^{1,3}, E. Ferrero¹, R. Richiardone², S. Falabino³, D. Anfossi³, S. Trini Castelli³, and E. Carretto³

¹Dipartimento di Scienze e Tecnologie Avanzate, Università del Piemonte Orientale, Alessandria, Italy

²Dipartimento di Fisica Generale, Università di Torino, Italy

³C.N.R., Istituto di Scienze dell'Atmosfera e del Clima, Torino, Italy

Received: 19 December 2008 – Revised: 9 April 2009 – Accepted: 20 April 2009 – Published: 18 May 2009

Abstract. One year of continuous wind and turbulence measurements at three levels (5, 9 and 25 m) on a mast located in the suburb of the city of Turin were collected. Those recorded during April 2007 are analyzed and their main characteristics are presented and discussed. The analysis includes, at each level, mean, standard deviation, Skewness, Kurtosis for the 3-D wind components and sonic temperature. The integral time scales for the 3-D wind components are also computed and friction velocity and Monin-Obukhov length are determined as well. In particular, the wind standard deviation profiles as a function of stability are compared to the literature predictions for flat undisturbed terrain. It is found that, while the vertical component agrees reasonably well, the horizontal components deviate from the prescribed values, as expected considering the buildings and other obstacles effects and the high percentage of low-wind conditions. Also the integral time scales, estimated by the autocorrelation functions, are compared to the literature predictions, finding significant differences, again attributed to the low-wind speed occurrences.

1 Introduction

The understanding of atmospheric turbulence in the urban canopy is very important for pollutant dispersion studies. There are strong similarities to atmospheric turbulence over plant canopies, but a consistent picture of urban canopy turbulence has not been achieved (see Rotach, 1999; Roth, 2000; Kastner-Klein and Rotach, 2004 for a review). Pollutant dispersion is difficult to predict in low wind, stable conditions, which are however very common in the Po valley (Northern Italy). In these conditions the turbulent and the dispersion characteristic parameters can be very different from those present in rural area. A review of the main results about low wind in the boundary layer and the related dispersion condition can be found in Anfossi et al. (2005). To investigate these peculiar conditions a one year field campaign has been conducted in the city of Turin, and the preliminary analysis of wind data measured in the outskirts of

the town is here described. This work focuses on the analysis of the turbulence and dispersion variables in the urban environment and on the evaluation of their parameterizations for modelling purposes. Two turbulence parameterizations, used in advanced atmospheric models for the Lagrangian Time-Scale and for the turbulent velocity fluctuations (Hanna, 1982; Degrazia et al., 2000), are tested. The Hanna (1982) parameterisation provides the turbulence profiles as a function of the surface layer and boundary layer parameters and proposes different expressions for the variances and for the Lagrangian time scales, distinguishing the different kinds of atmospheric stratification conditions, the unstable, stable and neutral cases. The method suggested by Degrazia et al. (2000) derives expressions for variances and decorrelation timescales, on the basis of Taylor's statistical diffusion theory and observed spectral properties, and provides their profiles as continuous values in the PBL at all elevations and all stability conditions. The analytical relation



Correspondence to: L. Mortarini
(l.mortarini@isac.cnr.it)



Figure 1. Satellite view of the measurement area. The blue circle indicates the mast.

between the wind velocity high order moments is studied and a dependence of the Kurtosis on Skewness is investigated in the various stability conditions. The auto-correlation functions of the 3-D wind components are evaluated to characterize the low-wind horizontal meandering.

2 The field campaign

The data were continuously collected (from 18 January 2007 to 19 March 2008) at the urban meteorological station of the Dipartimento di Fisica Generale at the University of Turin, in the southern outskirts of Turin, Italy (Lat.: $45^{\circ}1'4.00''$ N; Lon: $7^{\circ}38'34.21''$ E; 240 m a.s.l.). The site is characterized by a horizontal grassland surrounded by trees and high (30–35 m, approximately) buildings at a distance of about 300 m in the northern side, and smaller constructions (max 15 m high) in a range of about 200 m in the other directions (Fig. 1). A 25 m mast is located at the center of the area. Standard measurements include soil temperature (at -5 , -10 , -15 , -25 , -35 , -55 cm), dry and wet bulb temperature at screen height, air temperature at 5, 9 and 25 m height, relative humidity at 25 m height, wind speed and direction at 25 m height, global radiation, underground heat flux (at -8 and -15 cm), pressure and pressure fluctuations, with periods from 5 s to 18 h and resolution from 0.2 Pa to 2.0 Pa, measured by a microbarometer (Richiardone, 1993). During the field campaign three sonic anemometers (Solent R2 model by Gill Instruments) were installed on booms at 5 m, 9 m and 25 m height on the mast. They measured at a 21 Hz rate the u ,

v , w components of wind velocity and the sound speed in calibrated UVW mode. KH20 krypton hygrometers (Campbell Scientific) were placed near each anemometer to measure humidity fluctuations, and the roll and pitch movements of the 25 m height anemometer were measured by two inclinometers (NS-1/P models by Planar, with 0.05° accuracy). The output signals of the hygrometers, the inclinometers and the microbarometer were sampled at a 21 Hz rate by means of the analogue input channels of the anemometers (Table 2). The data presented in this paper refer to the period ranging from 14 April 2007 to 1 May 2007 (508 h). During all this observation sub-period the weather conditions were steady enough to consider more than the 90% of the data collected a reliable set for our purposes. Both stable and unstable conditions are statistically well represented (Table 1). The Turin area is characterized by low-wind conditions, and 85% of the wind speed data presented are less than 1.5 m/s. Hereinafter this value would be used as low-wind threshold.

To determine the PBL height we use the vertical temperature profiles measured by the Meteorological Temperature Profiler (Kipp & Zonen, MTP-5HE) of the ARPA-Piemonte station located in the Turin centre. The diurnal PBL height is determined through the potential temperature vertical profile, considering its first minimum. At nighttime time we consider the PBL height as the height of the first maximum in the temperature vertical profile.

3 Data analysis

3.1 Estimated parameters

In our preliminary analysis the attention is mainly focused on the turbulence parameters which enter the numerical dispersion models as input. The final rationale of the analysis here preliminarily discussed is to provide new parameterizations of the turbulence closure models. All the statistics are evaluated considering subsets of 1 h (7200 data). The surface layer parameters estimated are u_* , w_* , z_i , θ_* , L , where L is the Monin-Obukhov length scale, from measurements at 5 m and the turbulence quantities calculated are σ_i , S_i , K_i (for $i=u, v, w$) at the three sonic anemometers levels (5 m, 9 m and 25 m). The 5m estimation was used after having verified that the Monin Obukhov lengths evaluated at the three heights are very similar, so the local scaling would have given the same results.

Although comparing the measurements to Hanna's results could be misleading because Hanna's parameterizations are valid above the canopy layer, our aim is to verify how the turbulence parameters depart from the usual parameterizations in the urban environment.

3.2 Turbulent velocity fluctuations

Figure 2 shows the 3-D measured turbulent velocity fluctuations versus the values estimated by the two turbulent

Table 1. Number of hours for each stability class.

height	$-2 < \frac{z}{L} < -1.6$	$-1.6 < \frac{z}{L} < -1.2$	$-1.2 < \frac{z}{L} < -0.8$	$-0.8 < \frac{z}{L} < -0.4$	$-0.4 < \frac{z}{L} < 0$
25 m	14	19	22	28	38
9 m	12	14	19	42	84
5 m	7	13	20	33	121
height	$0 < \frac{z}{L} < 0.4$	$0.4 < \frac{z}{L} < 0.8$	$0.8 < \frac{z}{L} < 1.2$	$1.2 < \frac{z}{L} < 1.6$	$1.6 < \frac{z}{L} < 2$
25 m	37	26	20	15	11
9 m	80	33	19	11	4
5 m	109	31	8	9	12

Table 2. Anemometer arrangement and linked instruments

Height	Anemometer	Anem. Model and S/N	Hygrom. Model and S/N	Inclinometers	Microbarometer
25 m	160	Solent 1012R2A-0059	Campbell KH20-1132	yes	no
9 m	161	Solent 1012R2-0134	Campbell KH20-1235	no	no
5 m	162	Solent 1012R2-0144	Campbell KH20-1307	no	yes

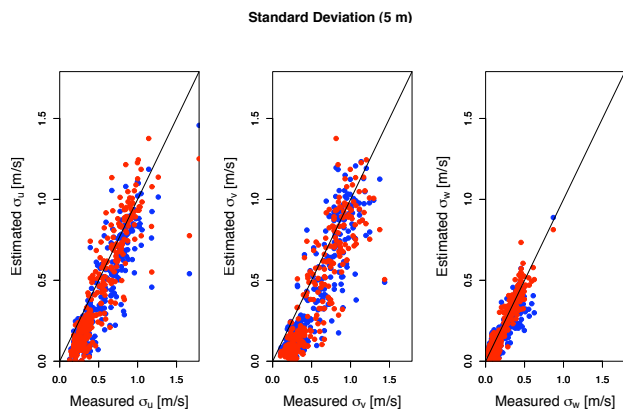


Figure 2. 3-D measured turbulent velocity fluctuations versus the values estimated by: • Degrazia et al. (2000) parametrization, • Hanna (1982) parametrization.

parameterizations. All the three components show a rather wide spread around the line of perfect agreement. Although the general behaviour is similar, they both under-estimate the measured values of the horizontal components, on which, for low-wind episodes, the meandering of the plume has a strong influence. These discrepancies may also be attributed to the complex geometry of the urban site, as a matter of fact the analytical relations are derived for flat terrain and may not be applicable in the urban environment.

In Fig. 3 normalized velocity standard deviations as a function of the stability parameter z/L are presented. While

for unstable, convective conditions ($z/L < 0$) measurements, parameterizations and analytical behaviours are in good agreement, in stable conditions ($z/L > 0$) the parametrized data underestimate both field data and the best fits of Moraes et al. (2005), Nieuwstadt (1984) and Smedman (1988). It should be noted that both the normalizations of the horizontal and vertical axis contain the parameter u^* , which can introduce a self-correlation (Baas et al., 2006). Though this is a preliminary result, it shows that the considered turbulence parameterization may not be adequate for stable conditions.

3.3 Eulerian time auto-correlation functions

The Eulerian time auto-correlation functions are evaluated from 1-h datasets. Figure 4a shows the correlation function:

$$R_i^E(\tau) = \frac{\overline{u_i(t)u_i(t+\tau)}}{\sigma_{u_i}(t)} \tag{1}$$

and it corresponds to a case of stronger wind. In this case it assumes the following well-known exponential form:

$$R_i^E(\tau) = e^{-\frac{\tau}{T_E}} \tag{2}$$

In the low wind speed case $R_i^E(\tau)$ shows a different behaviour (Fig. 4b), described by the following equation:

$$R_i^E(\tau) = e^{p\tau} \cos(q\tau) \tag{3}$$

where p and q are related to the Eulerian time scale T_E through:

$$T_E = \int_0^\infty R_i^E(\tau) d\tau = \frac{p}{p^2 + q^2} \tag{4}$$

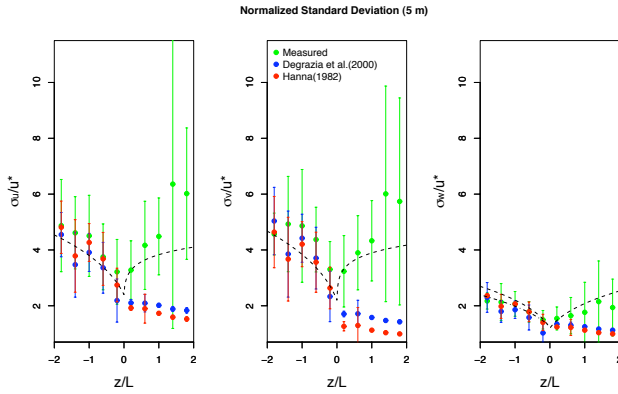


Figure 3. Normalized velocity standard deviations as a function of the stability parameter z/L . • Degrazia et al. (2000) parametrization, • Hanna (1982) parametrization, • measured data. The dotted line represents Moraes et al. (2005) best fit, while the dotted-point line (lower-left part of the right panel) represents Nieuwstadt (1984) and Smedman (1988) analytical formula.

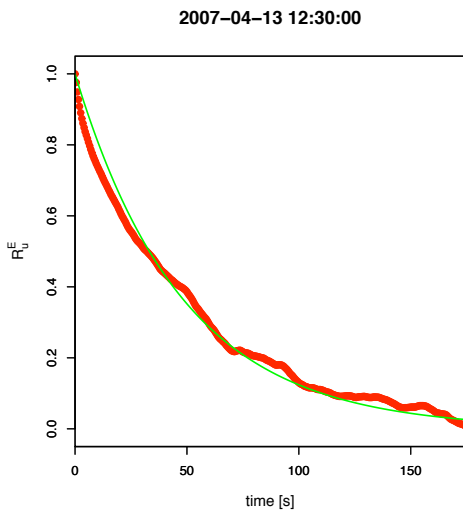


Figure 4a. Typical correlation function in the case of stronger wind at 25 m height. $\langle u \rangle = 1.85$ m/s.

and q represents the meandering parameter (Anfossi et al., 2005). In this subset of data, the percentage of meandering-type observations (< 1.5 m/s) is about 95% at 5 m and 53% at 25 m; this percentage is in accordance with Anfossi et al. (2005) analysis, where a 70% of low-wind conditions are attributed to the wind regime in the Po valley. Figure 4a and b reports two cases of almost perfect agreement between data and theoretical predictions. However, in the majority of cases it is difficult to find a universal behaviour for the auto-correlation functions. This occurs because $R_i^E(\tau)$ is not only a balance between the exponential decay and the oscillations due to the meandering, but it is also affected by non-stationary effects. The Eulerian Time-Scales are evaluated

2007-04-14 00:30:00

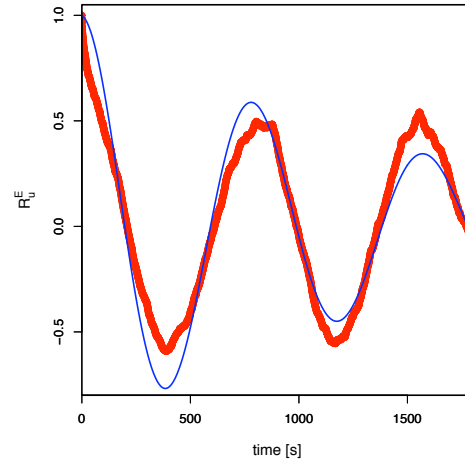


Figure 4b. Typical correlation function in the case of low wind at 5 m height. $\langle u \rangle = 0.23$ m/s.

both from best fits (making an assumption on the behaviour of the auto-correlation function) and from the integral (no assumption) of $R_i^E(\tau)$.

3.4 Lagrangian time scale

The Lagrangian time scales T_{Li} were estimated from the Eulerian ones T_{Ei} using the following relationship (Degrazia and Anfossi, 1998):

$$\frac{T_{Li}}{T_{Ei}} = \beta_i \tag{5}$$

where the T_{Ei} were obtained from the R_i^E and $\beta_i = 0.55 \frac{\langle U \rangle}{\sigma_i}$, being $\langle U \rangle$ the mean wind velocity.

Measured Lagrangian Time Scale and parametrized Lagrangian Time Scale ratio for the three different anemometers heights are presented in Fig. 5a, b and c. While in the σ_i (Fig. 2) determination the two parameterizations behave in the same way, for the T_L they show different estimated values. The Hanna (1982) parameterization works well for the lower heights in the vertical component, but it over-estimates T_L at 25 m, where probably the surrounding buildings effects is more effective. Both the parameterizations fail to correctly predict the horizontal Lagrangian Time-Scale, under-estimating it in unstable conditions and over-estimating it for stable ones. The failure of the parameterizations on the horizontal components can be interpreted considering that their scales of motion show a strong dependence on the topography and the geometry of the site, moreover, in stable conditions, the considered parameterizations does not account for the wind meandering. However a final statement can be given after a further investigation on the full data set.

It can also be noticed that the Hanna (1982) parameterization is in general showing a satisfactory agreement for

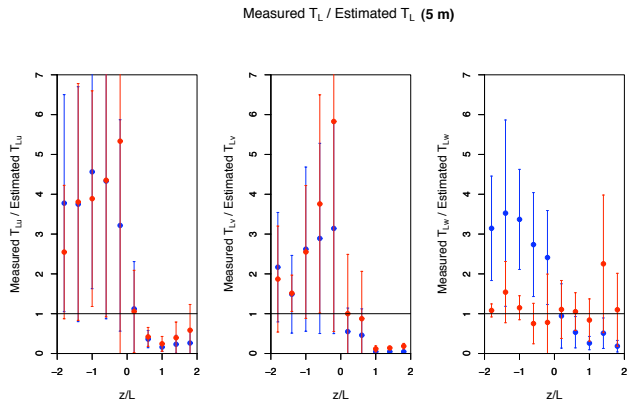


Figure 5a. Measured Lagrangian Time Scale and parametrized Lagrangian Time Scale ratio for the 5 m anemometer. ● Degrazia et al. (2000) parametrization, ● Hanna (1982) parametrization.

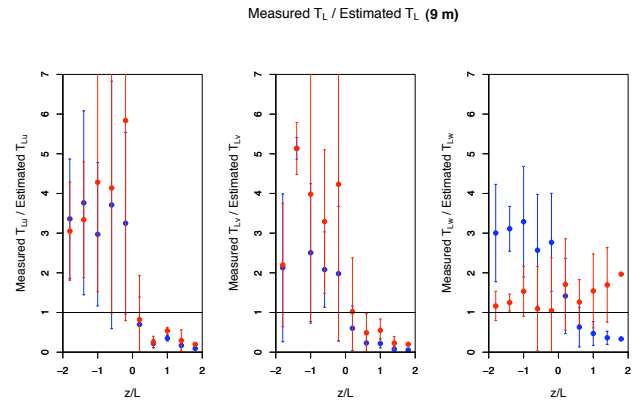


Figure 5b. Measured Lagrangian Time Scale and parametrized Lagrangian Time Scale ratio for the 9 m anemometer. ● Degrazia et al. (2000) parametrization, ● Hanna (1982) parametrization.

the vertical T_L . The different performances of Hanna (1982) and Degrazia et al. (2000) in the vertical component can be explained considering that the theory behind Degrazia et al. (2000) parameterizations is only based on the bulk structure of the PBL and it is not adjusted at the surface, while the Hanna (1982) parameterization, as well based on the bulk properties of the PBL, is adjusted near the surface, as far as we know using best fit analysis of data.

Figure 6a and b shows the daily evolution of the measured and estimated Lagrangian Time-Scales. Here it can be more clearly seen that, with the exception of Hanna (1982) estimation of the vertical Time-Scales, the parametrized T_L shows an opposite behaviour to the measured data. Surprisingly, the measured and estimated T_L differ also in unstable conditions (around noon), where the turbulence is expected to be mainly determined by convection. Even in these cases the complexity of the terrain and therefore the mechanical sources of turbulence have to be considered.

3.5 High-Order Statistics

The importance of high-order statistics for the turbulent dispersion is discussed in Wyngaard and Weil (1991) and Maurizi (2006).

In the (S, K) space an inferior limit for the Kurtosis (K) exists: $K=(S^2+1)$, which bounds the Quasi-Normal Approximation in the range of the Skewness (S) values. Tampieri et al. (2000) proposed the relation:

$$K = \alpha(S^2 + 1) \tag{6}$$

with $\alpha=3.3$ for a shear flow. Maurizi (2006) demonstrated that K-values above this curve correspond to damping terms for the turbulent kinetic energy (dynamic stability) and related these values to stable conditions, suggesting a dependence of $\alpha(\frac{z}{L})$ on the stability.

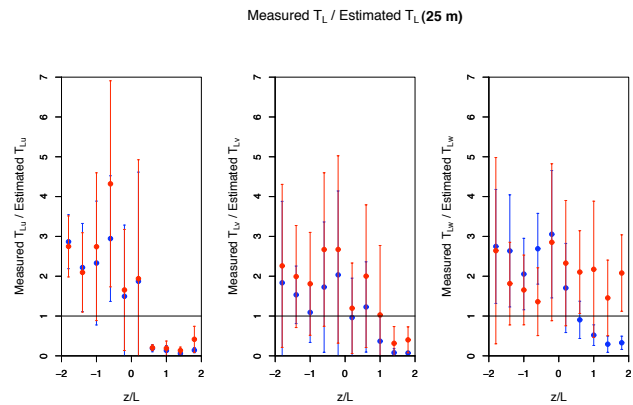


Figure 5c. Measured Lagrangian Time Scale and parametrized Lagrangian Time Scale ratio for the 25 m anemometer. ● Degrazia et al. (2000) parametrization, ● Hanna (1982) parametrization.

In Fig. 7a and b the vertical velocity Kurtosis as a function of the Skewness is depicted for low and stronger wind conditions respectively. The low wind case does not show any evidence of a parabolic dependence.

In Fig. 8a and b Kurtosis as a function of the Skewness is depicted for unstable and stable conditions respectively. The stable case, related to low wind conditions, does not show any evidence of a parabolic dependence. In stable conditions $K-S$ data are spread and do not show any analytical relationship.

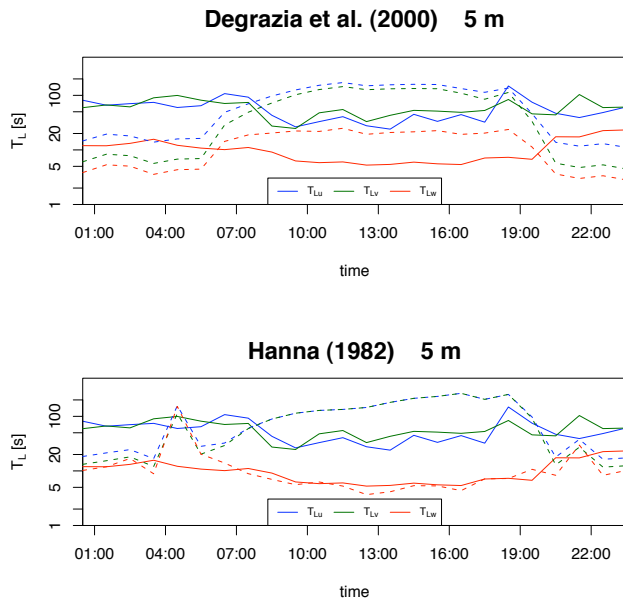


Figure 6a. Daily evolution of the measured (continuous lines) and estimated (dotted lines) Lagrangian Time-Scales for the 5 m anemometer. The error bars represent one standard deviation.

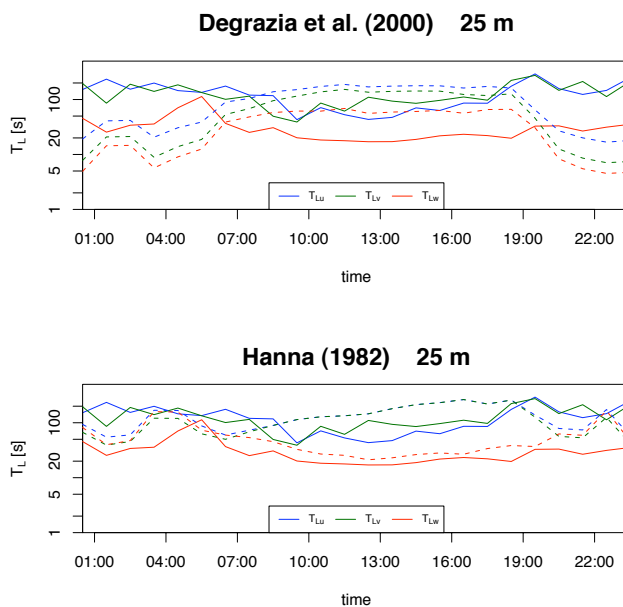


Figure 6b. Daily evolution of the measured (continuous lines) and estimated (dotted lines) Lagrangian Time-Scales for the 25 m anemometer. The error bars represent one standard deviation.

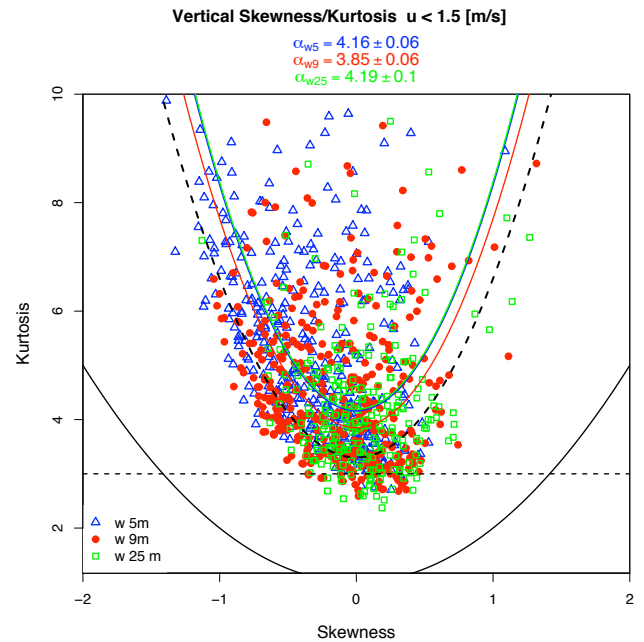


Figure 7a. Kurtosis as a function of the Skewness for low wind conditions. Δ 5 m data, \bullet 9 m data, \square 25 m data. The dotted parabola represents Maurizi (2006) best fit, the black one is the theoretical inferior limit, while the dotted line is the Gaussian limit. The coloured dotted lines are data best fits using formula (Eq. 6). The evaluated values of α_i ($i=5, 9, 25$) are shown at the top of the plot.

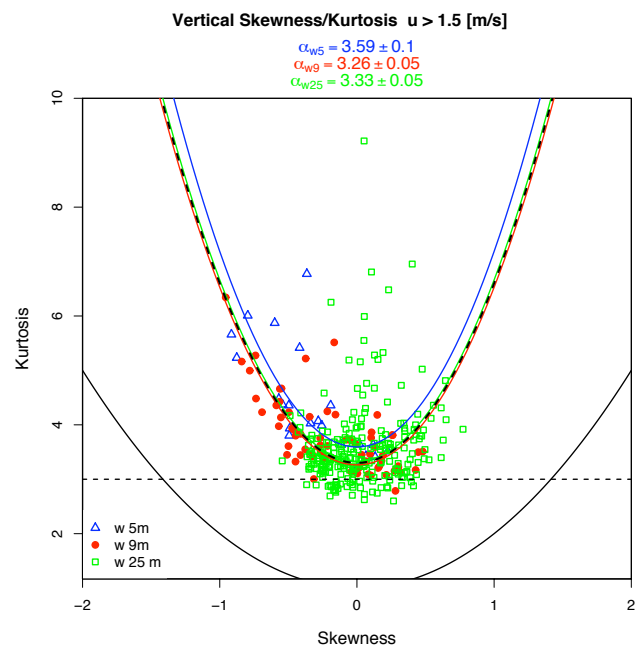


Figure 7b. Kurtosis as a function of the Skewness for strong wind conditions. Δ 5 m data, \bullet 9 m data, \square 25 m data. The dotted parabola represents Maurizi (2006) best fit, the black one is the theoretical inferior limit, while the dotted line is the Gaussian limit. The coloured dotted lines are data best fits using formula (Eq. 6). The evaluated values of α_i ($i=5, 9, 25$) are shown at the top of the plot.

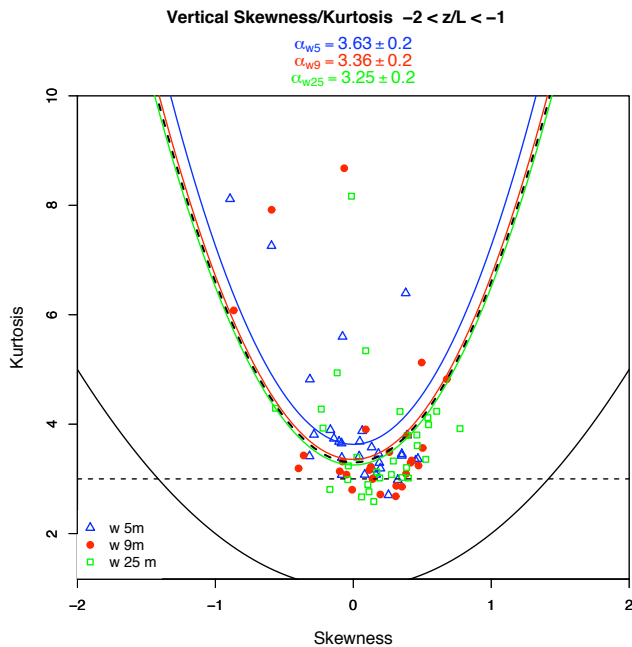


Figure 8a. Kurtosis as a function of the Skewness for unstable conditions. Δ 5 m data, \bullet 9 m data, \square 25 m data. The dotted parabola represents Maurizi (2006) best fit, the black one is the theoretical inferior limit, while the dotted line is the Gaussian limit. The coloured dotted lines are data best fits using formula (Eq. 6). The evaluated values of α_i ($i=5, 9, 25$) are shown at the top of the plot.

4 Conclusions

Turbulence measurements in an urban environment have been carried out and a subset of data was used here for a first test of two well-known turbulent parameterizations (Hanna, 1982; Degrazia et al., 2000). The measured velocity standard deviations follows the Moraes et al. (2005) best fits, while the two considered parameterizations Hanna (1982), Degrazia et al. (2000) underestimate the observations in stable conditions. Hanna (1982) T_L estimates satisfactorily fit the measured value for the vertical wind component. Both parameterizations, as expected, are not able to take into account the urban environment. In particular, the Lagrangian Time-Scale daytime behaviour of the horizontal components is almost opposite to the parametrized ones. Our results, showing that the Hanna and Degrazia parameterizations do not completely agree with the measured turbulence in the urban canopy, demonstrate, according to Roth (2000) suggestions, that some correction should be introduced in order to take into account the wake turbulence, even though the urban canopy, analogously to the plant canopy, shows many similarities to the plane mixing-layer flows. Further research is required, and is under process, to have the possibility of proposing higher-order parameterisations that can be profitably used in practical applications. As far as the High Order Moments are concerned, for low-wind conditions it is diffi-

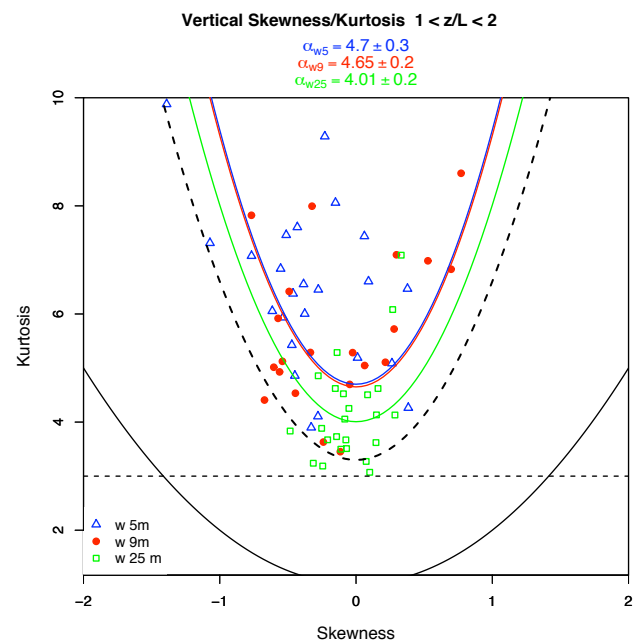


Figure 8b. Kurtosis as a function of the Skewness for stable conditions. Δ 5 m data, \bullet 9 m data, \square 25 m data. The dotted parabola represents Maurizi (2006) best fit, the black one is the theoretical inferior limit, while the dotted line is the Gaussian limit. The coloured dotted lines are data best fits using formula (Eq. 6). The evaluated values of α_i ($i=5, 9, 25$) are shown at the top of the plot.

cult to assume a parabolic dependence of the Kurtosis on the Skewness. The wind velocity vertical component shows a dynamic stability for low-wind and for stable conditions.

Acknowledgements. This work was funded by Regione Piemonte in the frame of the *Ricerca 2004* project. We would like to thank ARPA Piemonte for kindly providing us with meteorological data.

Edited by: P. J. H. Bultjes and M. Piringer
Reviewed by: two anonymous referees

References

- Anfossi, D., Oetl, D., Degrazia, G., and Goulart, A.: An analysis of sonic anemometer observations in low-wind speed conditions, *Bound.-Lay. Meteorol.*, 114, 179–203, 2005.
- Baas, P., Steeneveld, G. J., van de Wiel, B. J. H., and Holtslag, A. A. M.: Exploring self-correlation in flux-gradient relationships for stably stratified conditions, *J. Atmos. Sci.*, 63, 3045–3054, 2006.
- Degrazia, G. and Anfossi, D.: Estimation of the Kolmogorov constant C_0 from classical statistical diffusion theory, *Atmos. Environ.*, 32, 3611–3614, 1998.
- Degrazia, G., Anfossi, D., Carvalho, J., Mangia, C., Tirabassi, T., and Campos Velho, H.: Turbulence parameterisation for PBL dispersion models in all stability conditions, *Atmos. Environ.*, 34, 3575–3583, 2000.

- Hanna, S.: Applications in air pollution modelling, in: *Atmospheric Turbulence and Air Pollution Modelling*, edited by: Nieuwstadt, F. and Van Dop H., Reidel, Dordrecht, 275–310, 1982.
- Maurizi, A.: On the dependence of third- and fourth-order moments on stability in the turbulent boundary layer, *Nonlin. Processes Geophys.*, 13, 119–123, 2006, <http://www.nonlin-processes-geophys.net/13/119/2006/>.
- Moraes, O., Acevedo, O., Degrazia, G., Anfossi, D., da Silva, R., and Anabor, V.: Surface layer turbulence parameters over a complex terrain, *Atmos. Environ.*, 39, 3103–3112, 2005.
- Nieuwstadt, F.: The turbulent structure of the stable nocturnal boundary layer, *J. Atmos. Sci.*, 41, 2202–2216, 1984.
- Richiardone, R.: The transfer function of a differential microbarometer, *J. Atmos. Ocean. Tech.*, 10, 624–628, 1993.
- Rotach, M. W.: On the influence of the urban roughness sublayer on turbulence and dispersion, *Atmos. Environ.*, 33, 4001–4008, 1999.
- Kastner-Klein, P. and Rotach, M. W.: Mean flow and turbulence characteristics in an urban roughness sublayer, *Bound.-Lay. Meteorol.*, 111, 55–84, 2004.
- Roth, M.: Review of atmospheric turbulence, *Q. J. Roy. Meteor. Soc.*, 126, 941–990, 2000.
- Smedman, A.: Observations of a multi-level turbulence structure in a very stable boundary layer, *Bound.-Lay. Meteorol.*, 44, 231–253, 1988.
- Tampieri, F., Maurizi, A., and Alberghi, S.: Lagrangian models of turbulent dispersion in the atmospheric boundary layer, in *Ingegneria del vento in Italia 2000*, INVENTO 2000 Proceedings, 37–50, 2000.
- Wyngaard, J. C. and Weil, J. C.: Transport asymmetry in skewed turbulence, *Phys. Fluids A*, 3, 155–162, 1991.